Optimized Verlet-like algorithms for molecular dynamics simulations

I. P. Omelyan,[1] I. M. Mryglod,[1,2] and R. Folk[2]
[1]*Institute for Condensed Matter Physics, 1 Svientsitskii Street, UA-79011 Lviv, Ukraine*
[2]*Institute for Theoretical Physics, Linz University, A-4040 Linz, Austria*
(Received 29 October 2001; published 17 May 2002)

Explicit velocity- and position-Verlet-like algorithms of the second order are proposed to integrate the equations of motion in many-body systems. The algorithms are derived on the basis of an extended decomposition scheme at the presence of a free parameter. The nonzero value for this parameter is obtained by reducing the influence of truncated terms to a minimum. As a result, the proposed algorithms appear to be more efficient than the original Verlet versions that correspond to a particular case when the introduced parameter is equal to zero. Like the original versions, the extended counterparts are symplectic and time reversible, but lead to an improved accuracy in the generated solutions at the same overall computational costs. The advantages of the optimized algorithms are demonstrated in molecular dynamics simulations of a Lennard-Jones fluid.

DOI: 10.1103/PhysRevE.65.056706 PACS number(s): 02.60.Cb, 02.70.Ns, 05.10.−a, 95.75.Pq

The method of molecular dynamics (MD) is a powerful tool for the prediction and study of various phenomena in physics, chemistry, and biology. In MD simulations we deal with the necessity to solve numerically the equations of motion for a many-body system composed of interacting particles. The most of traditional algorithms, such as Runge-Kutta and predictor-corrector schemes [1,2], are usually unsuitable for integration of the resulting differential equations, because the solutions obtained exhibit a high instability on MD scales of time [3].

A variety of alternative algorithms were proposed and implemented over the years [4–8]. These include the well-known velocity-Verlet (VV) integrator [7]. This second-order integrator is employed in the great majority of MD simulations due to its simplicity and exceptional stability. Moreover, the VV algorithm is symplectic, time reversible, and able to reach a high level of accuracy with minimal number of force evaluations per time step [3,8]. In addition, the VV approach can be modified to integrate not only translational motion in atomic systems, but also simulate more complicated molecular and spin liquids [9–12].

The question of how to improve the efficiency of integration for atomic systems with long-range interactions has also been considered. As a result, so-called multiple time scale integrators have been introduced [13,14]. In these integrators, the additional slow subdynamics is treated in a specific way using the weakness of the long-range forces. The faster motion, caused by the interactions at short interparticle distances, remains to be integrated with the help of usual basic algorithms, such as VV integrator, for instance.

In the present paper we show that even within the basic consideration of translational motion (when additional splitting of interaction potentials into multiple scale components is no longer allowed), the VV algorithm presents, in fact, only a particular case among a whole family of symplectic reversible integrators of the second order. This case appears to be not so optimal, and more efficient second-order algorithms are possible.

The equations of motion for a classical system consisting of N particles can be cast in the following compact form:

$$\frac{d\boldsymbol{\rho}}{dt}=L\boldsymbol{\rho}(t), \tag{1}$$

where $\boldsymbol{\rho}\equiv\{\mathbf{r}_i,\mathbf{v}_i\}$ denotes the full set ($i=1,2,\ldots,N$) of phase variables with $\mathbf{r}_i$ and $\mathbf{v}_i$ being the position and velocity, respectively, of the ith particle, L is the Liouville operator,

$$L=\sum_{i=1}^{N}\left(\mathbf{v}_i\cdot\frac{\partial}{\partial\mathbf{r}_i}+\frac{\mathbf{f}_i}{m}\cdot\frac{\partial}{\partial\mathbf{v}_i}\right)\equiv A+B, \tag{2}$$

$\mathbf{f}_i=-\Sigma_{j(j\neq i)}^{N}\varphi'(r_{ij})\mathbf{r}_{ij}/r_{ij}$ designates the force acting on the particles of mass m each, due to the interactions described by the potential $\varphi(r_{ij})$, and $\mathbf{r}_{ij}=\mathbf{r}_i-\mathbf{r}_j$. The Liouville operator has been split in Eq. (2) into the free-motion $A=\mathbf{v}\cdot\partial/\partial\mathbf{r}$ and potential $B=\mathbf{f}/m\cdot\partial/\partial\mathbf{v}$ parts with $\mathbf{v}\equiv\{\mathbf{v}_i\}$, $\mathbf{r}\equiv\{\mathbf{r}_i\}$, and $\mathbf{f}\equiv\{\mathbf{f}_i\}$.

The formal solution of Eq. (1) is

$$\boldsymbol{\rho}(h)=e^{Lh}\boldsymbol{\rho}(0)\equiv e^{(A+B)h}\boldsymbol{\rho}(0), \tag{3}$$

where h denotes the time step. Of course, the exponential propagator e^{Lh} cannot be evaluated exactly at any h (solutions in quadratures are possible only for $N=2$ that is not relevant for our consideration of many-body systems when $N\gg 1$). However, at small enough values of h, the total propagator allows to be decomposed [15–18] as

$$e^{(A+B)h}=\prod_{p=1}^{P}e^{Aa_ph}e^{Bb_ph}+O(h^{K+1}), \tag{4}$$

where the coefficients a_p and b_p are chosen in such a way to provide the highest possible value for $K\geqslant 1$ at a given integer number $P\geqslant 1$. Then, starting from an initial configuration $\boldsymbol{\rho}(0)$, the evolution of the system can be investigated during arbitrary times t by repeating the single-step propagation, $\boldsymbol{\rho}(t)=(e^{Lh})^l\boldsymbol{\rho}(0)\equiv(e^{(A+B)h})^l\boldsymbol{\rho}(0)$, i.e.,

$$\boldsymbol{\rho}(t)=\left(\prod_{p=1}^{P}e^{Aa_ph}e^{Bb_ph}\right)^l\boldsymbol{\rho}(0)\equiv S(t)\boldsymbol{\rho}(0), \tag{5}$$

where $l=t/h$ is the total number of steps and the truncation terms $O(h^{K+1})$, appearing in Eq. (4), have been neglected.

The main advantage of decomposition (4) is that the exponential subpropagators $e^{A\tau}$ and $e^{B\tau}$ are analytically integrable. Indeed,

$$e^{A\tau}\boldsymbol{\rho}\equiv e^{\mathbf{v}\cdot\partial/\partial\mathbf{r}\tau}\{\mathbf{r},\mathbf{v}\}=\{\mathbf{r}+\tau\mathbf{v},\mathbf{v}\},$$
$$e^{B\tau}\boldsymbol{\rho}\equiv e^{\mathbf{f}/m\cdot\partial/\partial\mathbf{v}\tau}\{\mathbf{r},\mathbf{v}\}=\{\mathbf{r},\mathbf{v}+\tau\mathbf{f}/m\}, \tag{6}$$

which represent simple shifts of positions and velocities, respectively (with τ being equal to $a_p h$ or $b_p h$). In addition, the generated trajectory (5) behaves symplectically (like exact solutions), because such separate shifts do not change the volume in phase space. The time reversibility $S(-t)\boldsymbol{\rho}(t)=\boldsymbol{\rho}(0)$ of solutions [following from the property $S^{-1}(t)=S(-t)$ of evolution operators] can also be obtained by imposing additional conditions on the coefficients a_p and b_p. Namely, $a_1=0$, $a_{p+1}=a_{P-p+1}$, and $b_p=b_{P-p+1}$, or $a_p=a_{P-p+1}$, and $b_p=b_{P-p}$ at $b_P=0$. In other words, the subpropagators $e^{A\tau}$ and $e^{B\tau}$ should enter symmetrically in the decompositions. Then the even-order truncation terms $O(h^{2k})$ will disappear automatically in Eq. (4) at $k\leqslant K/2$. For this reason, the order K of reversible algorithms may accept only even numbers. The cancellation of odd-order terms $O(h^{2k-1})$ will be provided by satisfying a set of basic conditions for a_p and b_p. For example, the condition $\Sigma_{p=1}^{P}a_p=\Sigma_{p=1}^{P}b_p=1$ is required to cancel the first-order truncation uncertainties.

The method just highlighted is quite general to build numerical integrators of arbitrary orders. In particular, the second-order ($K=2$) VV algorithm

$$e^{(A+B)h}=e^{Bh/2}e^{Ah}e^{Bh/2}+O(h^3) \tag{7}$$

is immediately reproduced from Eq. (4) at $P=2$ and $a_1=0$, $b_1=b_2=1/2$, $a_2=1$. The case when the operators A and B are replaced by each other ($A\leftrightarrow B$) is also possible, and we come to the so-called position-Verlet (PV) algorithm [13], $e^{(A+B)h}=e^{Ah/2}e^{Bh}e^{Ah/2}+O(h^3)$, corresponding to the choice $a_1=a_2=1/2$, $b_1=1$, and $b_2=0$. Algorithms of higher orders can also be derived in a similar way. For instance, the fourth-order ($K=4$) algorithm by Forest and Ruth [16] is obtained from Eq. (4) at $P=4$, whereas sixth-order ($K=6$) schemes are derivable [15] beginning from $P=8$. The high-order schemes involve, however, too large number of force recalculations, and appear to be less efficient in most of MD applications than second-order algorithms.

Despite the fact that the method of construction of time-reversible integrators using symplectic decompositions is not new, some important cases have never been considered and have been completely ignored in the literature. This concerns, in particular, the following question. Are the above Verlet algorithms optimal in view of the time efficiency among all possible basic (i.e., with single splitting of the Liouville operator) decomposition integrators of the second order? We can say only that the Verlet algorithms do minimize the number of force evaluations per time step. However, as will be shown below, this does not guarantee the optimization with respect to the overall number of force recalculations (the most time-consuming part of MD simulations), which are necessary to perform during a fixed observation time in order to achieve a given precision in solutions.

It can be seen readily that the Verlet algorithms ($P=2$) require only one ($P-1$) force evaluation per time step h, whereas the fourth- and higher-order schemes ($P\geqslant 4$) need in three or more such evaluations. Let us consider now the intermediate case $P=3$ that leads to an extended time-reversible propagation in the form

$$e^{(A+B)h}=e^{A\xi h}e^{Bh/2}e^{A(1-2\xi)h}e^{Bh/2}e^{A\xi h}+Ch^3+O(h^4) \tag{8}$$

following from Eq. (4) at $a_1=a_3\equiv\xi$, $a_2=1-2\xi$, $b_1=b_2=1/2$, and $b_3=0$. Again, the propagation with $A\leftrightarrow B$ is also acceptable (then $a_1=0$, $b_1=b_3\equiv\xi$, $b_2=1-2\xi$, and $a_2=a_3=1/2$). Formula (8) represents a whole family of symplectic time-reversible integrators of the second order in which a particular member can be extracted by choosing a value for free parameter ξ. For $\xi=0$, Eq. (8) reduces to the VV [see Eq. (7)] or PV (at $A\leftrightarrow B$) algorithm. The extended (when $\xi\neq 0$) propagation requires already two, instead of one, force recalculation per time step. For this reason, we can come to an incorrect conclusion that such a propagation has no advantage over the Verlet algorithms.

In order to prove that the above conclusion is indeed incorrect, let us analyze in more detail the influence of truncation errors Ch^3 on the result. Expanding both the sides of Eq. (8) into Taylor's series with respect to h, one finds

$$C=\alpha(\xi)[A,[B,A]]+\beta(\xi)[B,[B,A]], \tag{9}$$

where

$$\alpha(\xi)=\frac{1-6\xi+6\xi^2}{12},\quad \beta(\xi)=\frac{1-6\xi}{24} \tag{10}$$

and $[,]$ denotes the commutator of two operators. The norm of C with respect to the third-order commutators $[A,[B,A]]$ and $[B,[B,A]]$ is

$$\gamma(\xi)=\sqrt{\alpha^2(\xi)+\beta^2(\xi)}. \tag{11}$$

Then the norm of local uncertainties $C\boldsymbol{\rho}h^3$ appearing in phase trajectory $\boldsymbol{\rho}$ during a single-step propagation given by Eqs. (3) and (8) can be expressed in terms of γ and h as $g=\gamma h^3$. During a whole integration over a fixed time interval t, the total number l of such single steps is proportional to h^{-1} [see Eq. (5)]. As a result, the local third-order uncertainties will accumulate step by step leading at $t\gg h$ to the second-order global errors $\Gamma=gh^{-1}$, i.e.,

$$\Gamma(\xi,h)=\gamma(\xi)h^2. \tag{12}$$

Extended propagation (8) can now be optimized with respect to ξ by minimizing the function $\gamma(\xi)$. As can be verified readily, the minimum of $\gamma(\xi)$ is achieved at $\xi=\zeta$, where

$$\zeta=\frac{1}{2}-\frac{(2\sqrt{326}+36)^{1/3}}{12}+\frac{1}{6(2\sqrt{326}+36)^{1/3}}$$
$$\approx 0.193\,183\,327\,503\,783\,6 \tag{13}$$

and consists $\gamma(\zeta)\approx 0.008\,55$. On the other hand, the value $\gamma(0)$ of γ corresponding to the Verlet algorithms (when $\xi=0$) is equal to $\gamma(0)\approx 0.0932$, i.e., it increases in $\gamma(0)/\gamma(\zeta)\approx 11$ times. Remembering that the extended propagation requires two force evaluation per time step h, it should be performed with double step size $2h$ with respect to that of the Verlet algorithms, in order to provide the same number of total force recalculations during the integration over the same time interval. Therefore, the extended propagation will be more efficient if the following inequality $\Gamma(\xi,2h)<\Gamma(\xi=0,h)$ takes place. Taking into account Eq. (12), such an inequality can be rewritten as $\gamma(0)/\gamma(\xi)>4$, and thus it is fulfilled completely in the optimization regime. In particular,

$$\frac{\Gamma(\zeta,2h)}{\Gamma(\xi=0,h)}\approx 0.367, \tag{14}$$

indicating that the optimized propagation, being applied even with double sizes of the time step, will reduce the global errors approximately in three times.

In view of Eqs. (3), (6), and (8), more explicit expressions for the single-step propagation of position and velocity from time t to $t+h$ within the optimized VV-like algorithm are:

$$\mathbf{r}_{\mathrm{I}}=\mathbf{r}(t)+\mathbf{v}(t)\xi h,$$
$$\mathbf{v}_{\mathrm{I}}=\mathbf{v}(t)+\frac{1}{m}\mathbf{f}(\mathbf{r}_{\mathrm{I}})h/2,$$
$$\mathbf{r}_{\mathrm{II}}=\mathbf{r}_{\mathrm{I}}+\mathbf{v}_{\mathrm{I}}(1-2\xi)h, \tag{15}$$
$$\mathbf{v}(t+h)=\mathbf{v}_{\mathrm{I}}+\frac{1}{m}\mathbf{f}(\mathbf{r}_{\mathrm{II}})h/2,$$
$$\mathbf{r}(t+h)=\mathbf{r}_{\mathrm{II}}+\mathbf{v}(t+h)\xi h,$$

whereas the optimized PV-like algorithm [when $A\leftrightarrow B$ in Eq. (8)] reads

$$\mathbf{v}_{\mathrm{I}}=\mathbf{v}(t)+\frac{1}{m}\mathbf{f}(\mathbf{r}(t))\xi h,$$
$$\mathbf{r}_{\mathrm{I}}=\mathbf{r}(t)+\mathbf{v}_{\mathrm{I}}h/2,$$
$$\mathbf{v}_{\mathrm{II}}=\mathbf{v}_{\mathrm{I}}+\frac{1}{m}\mathbf{f}(\mathbf{r}_{\mathrm{I}})(1-2\xi)h, \tag{16}$$
$$\mathbf{r}(t+h)=\mathbf{r}_{\mathrm{I}}+\mathbf{v}_{\mathrm{II}}h/2,$$
$$\mathbf{v}(t+h)=\mathbf{v}_{\mathrm{II}}+\frac{1}{m}\mathbf{f}(\mathbf{r}(t+h))\xi h,$$

where the parameter ξ should take its optimal value ζ [see Eq. (13)], and $\mathbf{r}_{\mathrm{I}}$, $\mathbf{r}_{\mathrm{II}}$, $\mathbf{v}_{\mathrm{I}}$, and $\mathbf{v}_{\mathrm{II}}$ are the auxiliary quantities denoting positions and velocities of all particles in intermediate stages. The algorithms are simple, require only slight modification with respect to the original Verlet versions, and can be easily implemented in program codes.

It is worth pointing out that the order of local errors $O(h^3)\equiv C\boldsymbol{\rho}h^3\equiv C\{\mathbf{r},\mathbf{v}\}h^3$ remains three in both position $\mathbf{r}(t+h)$ and velocity $\mathbf{v}(t+h)$ for both the optimized algorithms (15) and (16) [because the functions $\alpha(\xi)$ and $\beta(\xi)$ cannot tend to zero simultaneously at any ξ]. Note also that the minimization of third-order uncertainties Ch^3 in Eq. (8) automatically minimizes the fourth-order truncation terms $O(h^4)$ that are connected with C by the relation $O(h^4)=\frac{1}{2}[C(A+B)+(A+B)C]h^4+O(h^5)$. Further optimization is also possible in specific cases. For instance, some MD applications are aimed exclusively at the investigation of structural properties of the system. Then the accuracy of determining particle positions will play a more important role than that of velocities. In such a situation, it is quite natural to increase the precision in evaluation of $\mathbf{r}(t+h)$ by reducing the position part $C\mathbf{r}h^3=[\alpha(\xi)C_1+\beta(\xi)C_2]\mathbf{r}h^3$ of third-order truncation errors to zero, where $C_1=[A,[B,A]]$ and $C_2=[B,[B,A]]$ [see Eq. (9)]. This reduction can be realized, because (as can be shown using the explicit expressions for A and B) the operator C_2 vanishes when acting on position, i.e., $C_2\mathbf{r}=\mathbf{0}$, whereas $C_1\mathbf{r}\neq\mathbf{0}$ (as well as $C_1\mathbf{v}\neq\mathbf{0}$ and $C_2\mathbf{v}\neq\mathbf{0}$). The influence of $C_1\mathbf{r}$ can be reduced to zero also by choosing such ξ at which $\alpha(\xi)=0$. Among the two roots $(1\mp 1/\sqrt{3})/2$ of equation $\alpha(\xi)=0$, the preference should be given to the first of them, $(1-1/\sqrt{3})/2$, because it leads to a smaller value for $|\beta(\xi)|$. Then replacing ξ by $(1-1/\sqrt{3})/2$ in Eq. (15), we come to a positionally optimized VV-like algorithm in which the positions will be generated up to the fourth-order truncation uncertainties $O(h^4)$.

Another useful application of the positionally optimized algorithm is the case of weakly interacting systems, where the Liouville operator can be presented in the form $L=A+\epsilon B$ with $\epsilon\ll 1$. Then the operator $[B,[B,A]]\equiv C_2$, which forms the third-order errors in velocity, will be proportional to ϵ^2 and, thus, can be neglected. For the same reason, the corresponding fourth-order uncertainties $\frac{1}{2}[C_2(A+B)+(A+B)C_2)]h^4$ will also behave like ϵ^2. In such a case, the positionally optimized algorithm can be considered as a quasi-fourth-order integrator that, contrary to the usual fourth-order schemes, will require only two (instead of three) force evaluations per time step.

In order to obtain a positionally optimized algorithm within the PV-like integration (16), it is necessary simply to replace ξ by the root 1/6 of equation $\beta(\xi)=0$. Note that the values $1/6\approx 0.167$ and $(1-1/\sqrt{3})/2\approx 0.211$ are close enough to the optimal solution (13) that minimizes the total position-velocity uncertainties. Nevertheless, the positionally optimized algorithms are not recommended to be used in general case when both the position and velocity must be evaluated with a maximal accuracy. In other words, in such partially optimized algorithms the increased precision in position evaluation is achieved at the expense of decreasing

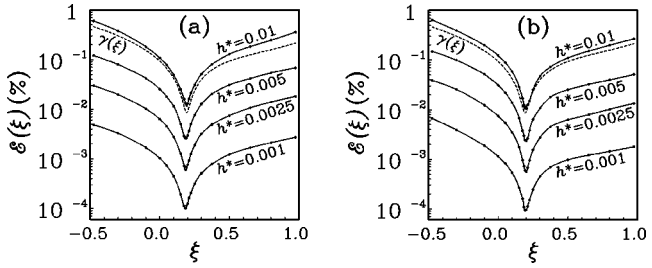

FIG. 1. The total energy fluctuations obtained in the simulations for different values of free parameter ξ at four reduced time steps, $h^*=0.01$, 0.005, 0.0025, and 0.001, using the VV [subset (a)] and PV [subset (b)] -like integration [Eqs. (15) and (16), respectively]. The simulation results are presented by circles connected by the solid curves. The function $\gamma(\xi)$ [see Eq. (11)] is plotted in both the subsets by the dashed curve.

accuracy in determining the velocities. Indeed, $\gamma(0)/\gamma(1/6)\equiv\gamma(0)/|\alpha(1/6)|\approx 7$ and $\gamma(0)/\gamma[(1-1/\sqrt{3})/2]\equiv\gamma(0)/|\beta[(1-1/\sqrt{3})/2]|\approx 8$ that is less than the factor $\gamma(0)/\gamma(\zeta)\approx 11$ corresponding to optimal value (13).

Our theoretical predictions were verified by testing the VV- and PV-like algorithms in MD simulations of a Lennard-Jones (LJ) fluid. We considered a system composed of $N=256$ particles interacting through the LJ potential $\Phi(r)=4u[(\sigma/r)^{12}-(\sigma/r)^6]$ in a basic cubic box of volume $V=L^3$ using periodic boundary conditions. The LJ potential was truncated at $r_c=L/2\approx 3.36\sigma$ and shifted to be zero at the truncation point to avoid the force singularities, i.e., $\varphi(r)=\Phi(r)-\Phi(r_c)$ at $r<r_c$ and $\varphi(r)=0$ otherwise. The simulations were carried out in a microcanonical ensemble at a reduced density of $n^*=(N/V)\sigma^3=0.845$ and a reduced temperature of $T^*=k_BT/u=1.7$. The equations of motion were integrated with the help of Eqs. (15) and (16) in which the parameter ξ, being constant within each run, varied from one run to another. All the runs started from an identical well equilibrated initial configuration $\boldsymbol{\rho}(0)$, and further continued $l=10\,000$ time steps. The precision of generated solutions was measured in terms of the relative total energy fluctuations $\mathcal{E}=\langle(E-\langle E\rangle)^2\rangle^{1/2}/|\langle E\rangle|$, where $E=\frac{1}{2}\Sigma_{i=1}^N m\mathbf{v}_i^2+\frac{1}{2}\Sigma_{i\neq j}^N\varphi(r_{ij})$ and $\langle\rangle$ denotes the microcanonical averaging. Note that in microcanonical ensembles the total energy is an integral of motion, $E(t)=E(0)$, and the above fluctuations should be equal to zero if the equations of motion are solved exactly. So that in approximate MD integration, smaller values of $\mathcal{E}$ will correspond to a more precise evaluation of phase trajectory.

The total energy fluctuations obtained in the simulations at the end of the runs for four (fixed within each run) dimensionless time steps, $h^*=h(u/m\sigma^2)^{1/2}=0.01$, 0.005, 0.0025, and 0.001, are shown in Fig. 1 as depending on free parameter ξ. The subsets (a) and (b) of this figure correspond to the VV- and PV-like integration, respectively. As can be seen, all the dependencies $\mathcal{E}(\xi,h)$ have one minimum that locates at the same point $\xi\approx 0.19$ independently on the size h of the time step. This point coincides completely with the minimum at ζ [Eq. (13)] of function $\gamma(\xi)$ [Eq. (11)] that is included in Fig. 1 as well (dashed curves in the subsets). Moreover, the energy fluctuations $\mathcal{E}(\xi,h)$ appear to be proportional to the

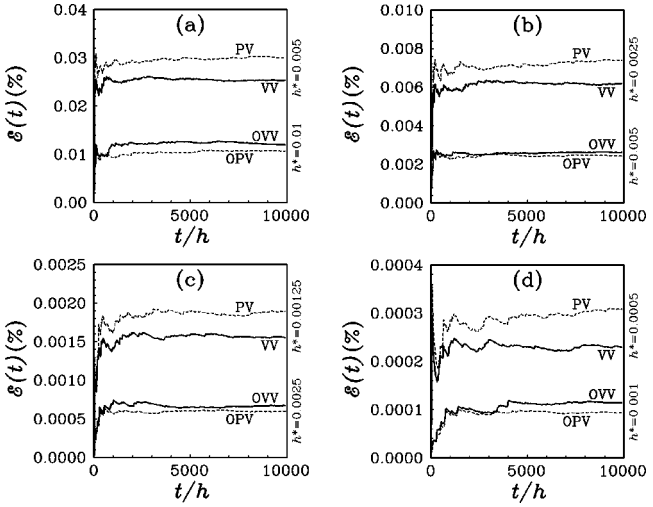

FIG. 2. The total energy fluctuations as functions of the length of the simulations performed using the optimized VV (solid curve marked as OVV) and PV (dashed curve, OPV) algorithms, as well as the original VV (solid curve, VV) and PV (dashed curve, PV) integrators. The results corresponding to different values of the time step, namely, $h^*=0.01$ and 0.005, 0.005 and 0.0025, 0.0025 and 0.00125, as well as 0.001 and 0.0005 are presented in subsets (a), (b), (c), and (d), respectively.

norm $\Gamma(\xi,h)$ of global errors [see Eq. (12)], and the coefficient of this proportionality almost does not depend on ξ and h. In addition, at each step size considered the energy fluctuations decrease at the minimum more than in ten times with respect to those at $\xi=0$, that is in agreement with our predicted value $\gamma(0)/\gamma(\zeta)\approx 11$.

The result for the total energy fluctuations as functions of the length of the simulations corresponding to the optimized (at $\xi=\zeta$) VV- and PV-like algorithms is presented in Fig. 2 at the same set of time steps. These functions are plotted by curves marked as OVV and OPV, respectively. For the purpose of comparison, the functions corresponding to the original VV and PV integrators are also drawn there (curves marked as VV and PV). Note that for the original integrators, the time step within each subset was chosen to be always twice smaller than that of the optimized versions (this condition is necessary to provide the same number of force recalculations during the same observation time), namely, $h^*=0.005$, 0.0025, 0.00125, and 0.0005 [see subsets (a), (b), (c), and (d), respectively]. Note also that within the original Verlet algorithms, the third- and higher-orders truncation uncertainties become too big at step sizes $h^*>0.005$. In particular, then the ratio of the total energy fluctuations to the fluctuations in potential energy (the standard ratio for estimating the precision of the calculations) appears to be more than a few percent. For this reason, such large step sizes cannot be used in precise MD simulations and, thus, are not considered in the present study.

As we see from Fig. 2, both the original (VV and PV) and optimized (OVV and OPV) algorithms exhibit very good stability properties (the excellent stability can be explained [3,8] by the symplecticity and time reversibility of the produced solutions). No systematic deviations in the total energy fluctuations can be observed for all the integrators. Instead, in each of the cases the amplitude of these deviations

tends to its own value that does not increase with further increasing the length of the simulations. However, this value appears to be significantly larger for the original versions VV and PV. On the other hand, using the optimized OVV and OPV algorithms even with double sizes of the time step allows us to decrease the unphysical energy fluctuations approximately in factor of 3. This is in an excellent accord with our theoretical prediction (14). Note also that the OPV algorithm is slightly better in energy conservation than its OVV version (whereas the VV integrator is better with respect to the PV counterpart). Furthermore, in view of the structure of Eqs. (15) and (16), the OPV algorithm is more convenient when averaging macroscopic quantities. In particular, then the interparticle potentials can be calculated at the end of time steps simultaneously with the interparticle forces within the same loop, increasing the time efficiency of the computations.

In conclusion, we point out that advanced second-order velocity- and position-Verlet-like algorithms have been proposed to improve the efficiency in MD simulations of classical systems. The algorithms are explicit (i.e., do not require any iteration), simple in implementation, and produce stable solutions that (like exact phase trajectories) are symplectic and time reversible. The main advantage of the introduced algorithms with respect to the widely used Verlet integrators is the possibility to generate more precise trajectories at the same overall computational efforts. As has been demonstrated in a particular case of microcanonical MD simulations of a LJ fluid, the proposed algorithms allow one to reduce in several times the unphysical fluctuations of the total energy.

It has been shown rigorously within a consequent theoretical approach that the proposed algorithms with respect to their time efficiency should be considered as optimal among all decomposition second-order integrators at single splitting of the Liouville operator. The optimized algorithms can be adapted to multiple scale integration (at the presence of long-range interactions when the potential part of the Liouville operator is decomposed additionally) and extended to many-component systems with orientational degrees of freedom. Moreover, the presented decomposition (8) of noncommutative operators is applicable for quantum Monte Carlo simulations [18] (because all the time coefficients at the exponential propagators remain positive in the optimized regime). These and other questions will be considered in further investigations.

Part of this work was supported by the Fonds zur Förderung der wissenschaftlichen Forschung under Project No. P15247-TPH. I.M. and I.O. thank the Fundamental Researches State Fund of the Ministry of Education and Science of Ukraine for support under Project No. 02.07/00303.

[1] C.W. Gear, *Numerical Initial Value Problems in Ordinary Differential Equations* (Prentice-Hall, Englewood Cliffs, NJ, 1971).
[2] R.L. Burden and J.D. Faires, *Numerical Analysis*, 5th ed. (PWS, Boston, 1993).
[3] M.P. Allen and D.J. Tildesley, *Computer Simulation of Liquids* (Clarendon, Oxford, 1987).
[4] L. Verlet, Phys. Rev. **159**, 98 (1967).
[5] D. Beeman, J. Comput. Phys. **20**, 130 (1976).
[6] R.W. Hockney and J.W. Eastwood, *Computer Simulation Using Particles* (McGraw-Hill, New York, 1981).
[7] W.C. Swope, H.C. Andersen, P.H. Berens, and K.R. Wilson, J. Chem. Phys. **76**, 637 (1982).
[8] D. Frenkel and B. Smit, *Understanding Molecular Simulation: From Algorithms to Applications* (Academic Press, New York, 1996).
[9] H.C. Andersen, J. Comput. Phys. **52**, 24 (1983).
[10] I.P. Omelyan, Comput. Phys. Commun. **109**, 171 (1998).
[11] I.P. Omelyan, Comput. Phys. **12**, 97 (1998).
[12] I.P. Omelyan, I.M. Mryglod, and R. Folk, Phys. Rev. Lett. **86**, 898 (2001).
[13] M. Tuckerman, B.J. Berne, and G.J. Martyna, J. Chem. Phys. **97**, 1990 (1992).
[14] S.J. Stuart, R. Zhou, and B.J. Berne, J. Chem. Phys. **105**, 1426 (1996).
[15] H. Yoshida, Phys. Lett. A **150**, 262 (1990).
[16] E. Forest and R.D. Ruth, Physica D **43**, 105 (1990).
[17] M. Suzuki and K. Umeno, in *Computer Simulation Studies in Condensed Matter Physics VI*, edited by D.P. Landau, K.K. Mon, and H.-B. Schüttler (Springer, Berlin, 1993).
[18] M. Suzuki, in *Computer Simulation Studies in Condensed Matter Physics VIII*, edited by D. P. Landau, K. K. Mon, and H.-B. Schüttler (Springer-Verlag, Berlin, 1995).